JOURNAL OF AIRCRAFT
Vol. 31, No. 4, July–Aug. 1994

Separation Bubble Model for Low Reynolds Number Airfoil Applications

Y. K. Shum* and D. J. Marsden†
University of Alberta, Edmonton, Alberta T6G 2G8, Canada

Midchord laminar separation bubbles, which act as a transition mechanism on low Reynolds number airfoils, make a contribution to wing section profile drag that becomes increasingly important at low Reynolds number. A model for the analysis of the boundary layer through the bubble is needed. The model developed here, which is based on Horton's method, provides a simple computationally efficient analysis that matches the integral boundary-layer analysis methods used on most existing boundary-layer codes. The bubble calculation is initiated by the detection of laminar separation. Transition location and boundary-layer growth in the laminar region are determined using Van Ingen's shortcut e^n method and Schmidt's correlations, respectively. Following Horton, the turbulent region is calculated using an iterative scheme that also functions as a bursting criterion, but the original linear velocity distribution has been replaced by Wortmann's concave velocity distribution. Both computation efficiency and prediction accuracy were improved after this change. Testing against experimental data showed that the bubble model greatly improved the drag prediction accuracy of the analysis in the Reynolds number range from 0.2 to 1.5 × 10^6, especially in cases when the midchord bubble was dominant. The validity of the bubble model was further confirmed by accurate prediction of bubble size and reattachment velocity gradient.

Nomenclature

B = laminar separation angle parameter
C_D = drag coefficient
C_d = dissipation integral, $2\int_0^\infty \tau(\partial u/\partial\eta)\,d\eta/(\rho u_e^3)$
C_f = skin friction coefficient, $[2\tau/(\rho u_e^2)]_{\eta=0}$
C_L = lift coefficient
c = chord
H_{12} = shape factor, δ_1/δ_2
H_{32} = shape factor, δ_3/δ_2
I = maximum amplification integral
l = total bubble length, $l_1 + l_2$
l_1 = length of bubble laminar region, $s_T - s_S$
l_2 = length of bubble turbulent region, $s_R - s_T$
m = velocity distribution exponent defined in Eq. (9)
n = exponential growth of Tollmien-Schlichting waves in the e^n method
Re_c = chord Reynolds number, $u_\infty c/\nu$
Re_s = distance Reynolds number, $u_\infty s/\nu$
$Re_{\delta 2}$ = momentum thickness Reynolds number, $u_e\delta_2/\nu$
s = distance along surface from stagnation point
Tu = freestream turbulence level
u = velocity component, tangential to surface
u_e = external velocity
x_b = position along the chord line
α = angle of attack
β = velocity distribution parameter used in Eq. (8)
δ_1 = displacement thickness, $\int_0^\infty (1 - u/u_e)\,d\eta$
δ_2 = momentum thickness, $\int_0^\infty (u/u_e)[1 - (u/u_e)]\,d\eta$
δ_3 = energy thickness, $\int_0^\infty (u/u_e)[1 - (u/u_e)^2]\,d\eta$
η = distance normal to airfoil surface
Λ = velocity gradient parameter, $(\delta_2/u_e)(du_e/ds)$
Λ_2 = Pohlhausen velocity gradient parameter, $(\delta_2^2/\nu)(du_e/ds)$
ν = kinematic viscosity
ρ = density
τ = shear stress

Subscripts
m = mean value
R = reattachment
S = separation
T = transition

Superscripts
$\bar{}$ = lengths and velocities normalized by δ_{2S} and u_{eS}, respectively
$\hat{}$ = lengths and velocities normalized by δ_{2T} and u_{eT}, respectively

Introduction

At low Reynolds number (especially $Re_c < 10^6$), a laminar flow generally separates when it encounters an adverse pressure gradient. The laminar shear layer becomes very unstable after separation. Once transition to turbulent flow takes place, the entrainment increases, causing reattachment to the airfoil surface. Depending on the amount of adverse pressure gradient and local Reynolds number at separation Re_s, the three processes 1) separation, 2) transition, and 3) reattachment, can happen in a few percent of chord length. The resulting flow structure is a short separation bubble. With increasing α, accompanied by steeper adverse pressure gradient and lower Re_c, the flow cannot reattach in a short distance, and so the bubble extends to become a long bubble. If the angle of attack continues to increase, the flow can eventually fail to reattach, and the bubble bursts. Both Ward,[1] and Tani[2] carried out an extensive survey of the experimental observations on the two types of bubbles and the bursting phenomenon. Notably, they classified a bubble that affects only the local pressure distribution as a short bubble, whereas a long bubble is classified as one that can cause the collapse of the suction peak, and consequently, the loss of lift.

Figure 1 illustrates the perturbation on the surface velocity distribution due to the presence of a bubble. The dashed line represents the external velocity u_e distribution when the bubble is eliminated by a boundary-layer trip, while the solid line represents the perturbed u_e distribution when the bubble is

Received Oct. 28, 1992; revision received April 25, 1993; accepted for publication July 21, 1993.
*Graduate Student, Department of Mechanical Engineering.
†Professor, Department of Mechanical Engineering.

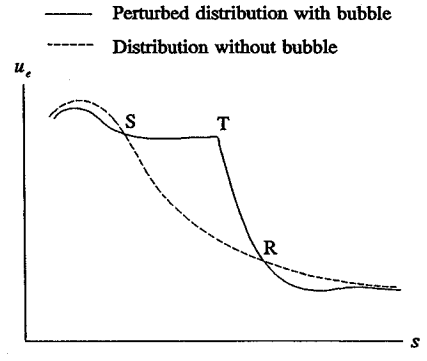

Fig. 1 Velocity distribution near a separation bubble.

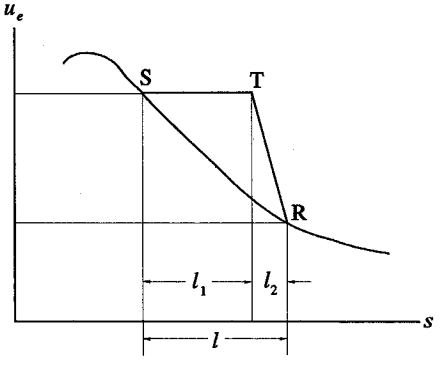

Fig. 2 Velocity distribution of Horton's bubble model.

present. The bubble case is characterized by the u_e distribution "plateau" between separation and transition. After transition, the turbulent entrainment causes the shear layer to reattach to the airfoil surface by having the flow decelerating quickly. In fact, the velocity gradient between T and R (solid line) is steeper than any segment of the attached flow u_e distribution (dashed line). The steep velocity gradient results in the intense growth of the turbulent shear layer.

Unless controlled by a turbulator,[3] bubbles can appear on an airfoil if it is operated at a Re_c lower than the design value. Moreover, some airfoil designers, including Marsden[4] and Drela,[5] deliberately use a short bubble as a transition mechanism. Due to the frequent occurrences of bubbles on airfoils operating at $Re_c < 10^6$, an airfoil analysis program can only predict drag accurately by simulating the boundary-layer growth inside a bubble. This article presents a simple bubble model which can be incorporated easily into an existing airfoil analysis program.

Original Horton's Method

The current bubble model is based on the one developed by Horton,[6] which was intended to investigate the bubble bursting phenomenon. If bursting does not happen and the separated flow reattaches to the airfoil surface, the model for boundary-layer growth in the separated region can be used to establish initial conditions for the subsequent turbulent boundary-layer calculation.

Horton's model is shown in Fig. 2. He assumes that there is no perturbation on the velocity distribution outside the bubble region. He also specifies that $u_{eT} = u_{eS}$, and $\delta_{2T} = \delta_{2S}$. Following Horton's notation, parameters normalized against separation condition will appear with an overline in the following text. For example, $\bar{u}_e$ represents u_e/u_{eS}.

The essence of Horton's method lies in the model of the turbulent shear layer and its reattachment. As illustrated in Fig. 2, Horton assumes that the turbulent shear layer decelerates linearly from T to R. Horton then calculates the boundary-layer growth in the turbulent region by integrating the following boundary-layer integral equation between T to R:

$$\frac{1}{u_e^3}\frac{\mathrm{d}}{\mathrm{d}s}(u_e^3 H_{32}\delta_2) = C_d \tag{1}$$

which results in a relationship between $\bar{u}_{eR}$ and $\bar{l}_2$:

$$\bar{u}_{eR}^4 = \frac{(C_{dm}/4H_{32m}) + [(1 - \bar{u}_{eR})/\bar{l}_2]}{(C_{dm}/4H_{32m}) - \Lambda_R} \tag{2}$$

After some minor adjustments to the theoretical values so that they can correspond better with the experimental data from various sources, Horton suggests the following:

$$\begin{aligned} \Lambda_R &= -0.0082 \\ H_{32m} &= 1.50 \\ C_{dm} &= 0.0182 \end{aligned} \tag{3}$$

Testing shows that Horton's model requires negligible computation time, but tends to underpredict the shear layer growth inside the bubble. The objective of the present investigation was to apply some of the advances made since 1967 in both experimental observation and theoretical analysis to upgrade Horton's model into a reliable tool for low Re_c airfoil analysis.

Modified Bubble Model

First, Horton's transition criterion is replaced by the shortcut e^n method developed by Van Ingen[7] as a compromise between computation ease and accuracy. It is based on the theory of Tollmien-Schlichting (TS) waves amplification in the laminar separated flow, thus the effect of freestream turbulence can be accounted for. On the other hand, it requires substantially less computation time than other more complicated applications of e^n method.[8,9] Van Ingen's shortcut e^n method can be summarized as follows:

$$I = \frac{10^4 B(-\Lambda_{2S})n_T}{Re_{\delta 2,S}} \tag{4}$$

$$z = \begin{cases} \dfrac{I - 122.5}{530} & I \le 646 \\ \left(\dfrac{I}{650}\right)^2 & I > 646 \end{cases} \tag{5}$$

$$l_1 = \frac{z\delta_{2S}Re_{\delta 2,S}}{B(-\Lambda_{2S})} \tag{6}$$

Van Ingen and Boermans[8] specifies B as 17.5, and n_T as a user-input parameter based on freestream turbulence level.

After determining the transition location, the laminar shear layer growth can be expressed in terms of the separation condition and l_1. The correlations chosen are those developed by Schmidt and Mueller,[10] who argue that the separated shear layer on an airfoil surface bears a strong resemblance to the free shear layer in terms of pressure gradient and velocity profile similarity. Therefore, by drawing analogy to the theoretical δ_2 growth in a free shear layer, they suggest that

$$\frac{\delta_{2T}}{\delta_{2S}} = \sqrt{1 + \frac{(1.241)^2 l_1}{\delta_{2S}Re_{\delta 2,S}}} \tag{7}$$

which completes the modifications on the laminar region model.

In view of Van Ingen and Boermans'[8] successful application of Stratford's[11,12] optimum recovery as bursting criterion, it was decided to adopt the similar but more flexible Wortmann's[13] recovery to model the turbulent shear layer in the current project. Although Wortmann's recovery was originally developed for attached flow on the verge of separation, it is likely that it is applicable to the turbulent region development with little error due to the shortness of the region. Nevertheless, the concave velocity distribution resulting from Wort-

mann's recovery certainly agrees better with experimental observation than the linear distribution proposed by Horton.

With the consideration that growth in the laminar region is substantial, variables will be normalized using transition condition (δ_{2T}, u_{eT}) rather than using separation condition as done by Horton. To avoid confusion, the superscript ˆ will be used from this point on to represent variables normalized against transition condition. For example, $\hat{u}_e$ represents u_e/u_{eT}.

With the new notation, the velocity distribution generated from Wortmann's recovery can be expressed as

$$\hat{u}_e = (u_e/u_{eT}) = [1 + \beta(\hat{s} - \hat{s}_T)]^{-m} \tag{8}$$

where

$$m = 0.33 - (0.074/6\beta Re_c^{0.2}) \tag{9}$$

At reattachment, Eq. (8) can be rewritten as

$$\hat{u}_{er} = (u_{eR}/u_{eT}) = (1 + \beta \hat{l}_2)^{-m} \tag{10}$$

which can be solved with the velocity distribution on the airfoil surface by an iterative scheme. Likewise, bursting is assumed to occur if the calculation fails to produce converged values of u_{eR} and l_2. Preliminary testing suggests that Eq. (10) is more successful in predicting bursting than Horton's method which fails to predict the occurrence of reattachment in some cases. Van Ingen et al.[8] observe the same trend when using the also concave Stratford velocity distribution.

Following Horton, the growth of the turbulent shear layer can be calculated by integrating Eq. (1) between T and R with Wortmann's velocity distribution, Eq. (8). After evaluating the integral, the following is obtained:

$$\frac{\delta_{2R}}{\delta_{2T}} = \hat{\delta}_{2R} = \frac{1}{\hat{u}_{eR}^3}\left\{1 + \frac{C_{dm}}{H_{32m}}\left[\frac{(1 + \beta \hat{l}_2)^{(-3m+1)} - 1}{\beta(-3m + 1)}\right]\right\} \tag{11}$$

Both u_{eR} and l_2 in Eq. (11) have been determined through the iterative scheme, leaving C_{dm}, H_{32m}, and β as the only unknowns. Horton suggests that $C_{dm} = 0.0182$, but Roberts[14] argues that Horton obtains the value in a condition where the velocity gradient is zero. Therefore, he suggests a much higher value of C_{dm} at 0.0350, which can account for the larger flow dissipation associated with the steep velocity gradient typical to the turbulent region. This is also supported by Schmidt et al.[10] who states that prediction of δ_2 can be more accurate using Robert's value for C_{dm}. However, numerical expressions from Drela and Giles,[15] and Dini[16] suggests that C_{dm} can vary considerably with Re_c. Thus, the dependence of C_{dm} on Re_c can only be found by incorporating the bubble model into an airfoil analysis program and then calibrating it with experimental data. On the other hand, there seems to be no objection to Horton's suggestion that $H_{32m} = 1.50$, so the same value was used in the current project.

Λ_R is no longer involved in the calculation after the introduction of Wortmann's velocity distribution, but its definition

$$\Lambda_R = \frac{\hat{\delta}_{2R}}{\hat{u}_{eR}}\left(\frac{d\hat{u}_e}{d\hat{s}}\right)_R = \frac{\hat{\delta}_{2R}}{\hat{u}_{eR}}\left[\frac{-m\beta}{(1 + \beta \hat{l}_2)^{(m+1)}}\right] \tag{12}$$

can provide a guideline for obtaining the value of β in Eq. (10). Schmidt et al.[10] suggests that Λ_R should range between -0.0099 and -0.0060, based on experimental results from O'Meara.[11] The bubble calculation is summarized in Fig. 3 for reference.

Compared to Dini's[16] calculation scheme which represents the most recent development on bubble model, the modified Horton's model is considerably simpler. This is because the iterative scheme in Horton's model is limited to the turbulent region, while Dini's model has its iterative scheme extended to cover the entire bubble. Dini claims that his model is more effective in simulating the upstream influence of bubble by communicating flow information from reattachment region upstream to the separation point. Although Dini's bubble model holds the advantage of better accuracy and computation stability, the current project will follow the more traditional scheme, which has iterative calculation confined in the turbulent region only. In other words, the state of the laminar region is calculated directly from the separation condition. Once determined, it cannot be altered by the subsequent development in the turbulent region. It is believed that this straightforward approach can still produce satisfactory results for engineering purposes and is in better coherence with the simplicity of Horton's method. Also, it is more efficient to "tune" an analysis program against experimental results if it involves fewer empirical parameters.

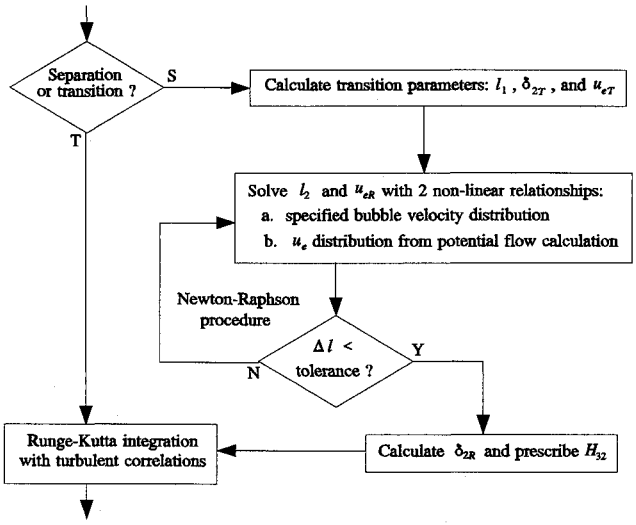

Fig. 3 Bubble calculation flow chart.

Incorporation Bubble Model into Airfoil Analysis

The current bubble model was incorporated into Kennedy's[17] airfoil analysis program which is based on viscous-inviscid interaction. The inviscid (potential) flow is calculated with a vortex panel method, and it produces airfoil velocity distribution and lift (C_L) as the outputs. The calculation has subsequently been modified by adding a source to the airfoil trailing edge to achieve better simulation of the displaced airfoil surface due to the presence of the boundary layer.

The viscous flow is calculated with the integral equations of subsonic boundary layers

$$\frac{d\delta_2}{ds} = \frac{C_f}{2} - (2 + H_{12})\frac{\delta_2}{u_e}\frac{du_e}{ds} \tag{13}$$

$$\frac{d\delta_3}{ds} = C_d - \frac{3\delta_3}{u_e}\frac{du_e}{ds} \tag{14}$$

The boundary-layer calculation for each surface starts at the stagnation point and proceeds downstream by integrating both Eqs. (13) and (14) simultaneously with Runge-Kutta second-order method. The location of the stagnation point has been determined from the potential flow solution. The closure correlations to Eqs. (13) and (14) are obtained from Eppler[18] for laminar flow, and Drela and Giles[15] for turbulent flow. Transition in attached flow is detected using the e^n method with correlation developed by Gleyzes et al.,[9] while laminar separation is detected using the criteria from Liu and Sandborn,[19] and Curle and Skan.[20] Airfoil drag C_D is then calculated by the widely used Squire and Young formula[21] which relates C_D to the trailing-edge, boundary-layer condition. As shown in

Fig. 4, the viscous calculation only requires the velocity distribution u_e around the airfoil as input, and produces two major outputs: 1) the airfoil drag coefficient C_D, and 2) displacement thickness δ_1 around the airfoil. Those δ_1 distributions are used for viscous-inviscid coupling. The bubble model was incorporated in the boundary-layer calculation by replacing the dashed line in Fig. 4.

The coupling of viscous and inviscid calculation is then achieved by iterative calculation. An equivalent airfoil representing the effect of viscous flow is simulated by displacing the original airfoil surface normally outward by an amount equal to the local δ_1 value produced from the boundary-layer calculation. Again, a new velocity distribution can be obtained from the equivalent airfoil coordinates using the panel method. After that, the three processes, 1) boundary-layer calculation, 2) equivalent airfoil simulation, and 3) the panel method, form an iteration loop. The looping is repeated until both C_L (from panel method), and C_D (from boundary-layer calculation) converge within their respective tolerances.

Calibration and Numerical Results

Since the two parameters, β and C_{dm}, are left open in the bubble model, it is necessary to calibrate them with experimental data on a trial and error basis and then verify the validity of the bubble model by applying it to other airfoils. The airfoils selected for calibration include Eppler 387,[22] FX 66-17A-175,[23] and FX 66-S-196 V1.[23] These data cover the Re_c range between 0.2–1.5 $\times$ 10^6. With Re_c higher than 1.5 $\times$ 10^6, the effect of bubble is so small that reliable data are not available for calibration. On the other hand, if Re_c drops below 0.2 $\times$ 10^6, the bubble generally extends to have substantial perturbation on the velocity distribution outside the bubble region. Reliable results using the current bubble model are not expected for such low Reynolds number.

The program was calibrated with the Eppler 387 airfoil at Re_c = 0.2 and 0.3 $\times$ 10^6. n_T is chosen as 11.2 for Tu = 0.055% according to Van Ingen and Boermans.[8] The reason for choosing β as 0.022 is that it gives the closest agreement between the calculated and the measured values of l and Λ_R, especially at Re_c = 0.3$\times$ 10^6. With β fixed at 0.022, the optimal value of C_{dm} can then be found on a trial and error basis. After some iterations the value of C_{dm} is chosen to be 0.017 at Re_c = 0.2 $\times$ 10^6, and 0.025 at Re_c = 0.3 $\times$ 10^6. Figure 5 shows a comparison of calculated and measured pressure distributions for the Eppler 387 at Re_c = 0.2 $\times$ 10^6 and α = 2 deg.

Calibration with the FX 66-17A-175 airfoil was done at Re_c = 10^6 and 1.5 $\times$ 10^6. n_T is chosen as 14 because Tu is less than 0.02% at the Laminar Wind Tunnel of University of Stuttgart (Stuttgart LWT). Again, based on the output Λ_R values, β is chosen to be 0.022. The optimal values of C_{dm} is found to be 0.055 at Re_c = 10^6 and 0.075 at Re_c = 1.5 $\times$ 10^6.

Calibration with the FX 66-S-196 V1 airfoil was done at Re_c = 0.5 $\times$ 10^6. Since the airfoil was tested in the Low Speed Laboratory at Delft University of Technology,[3] n_T was chosen as 11.2 following Van Ingen and Boermans.[8] Figure 6 shows that excellent results can be obtained by choosing β as 0.022, and C_{dm} as 0.035 at Re_c = 0.5 $\times$ 10^6. Results for the Eppler 387 airfoil at Re_c = 0.2 $\times$ 10^6 with β = 0.022 and C_{dm} = 0.087 in Fig. 7 also shows good agreement with experimental results at this lower Reynolds number.

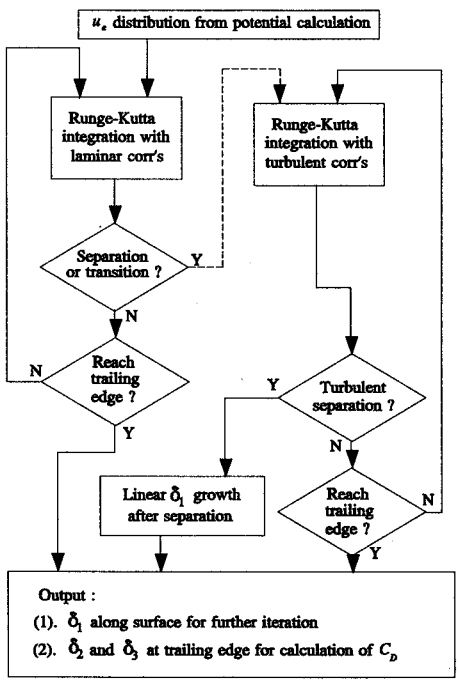

Fig. 4 Boundary-layer calculation flow chart.

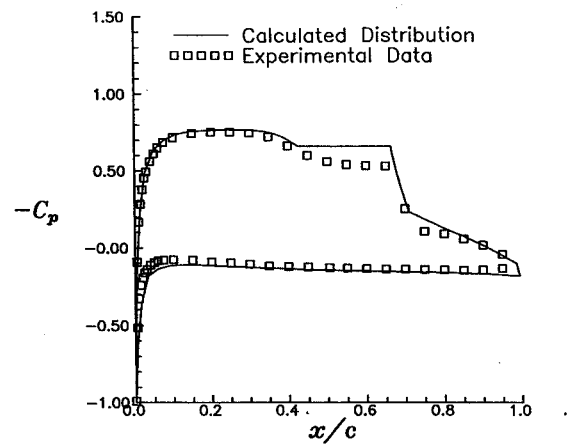

Fig. 5 Pressure distribution of Eppler 387 airfoil at Re_c = 0.2 $\times$ 10^6 and α = 2 deg.

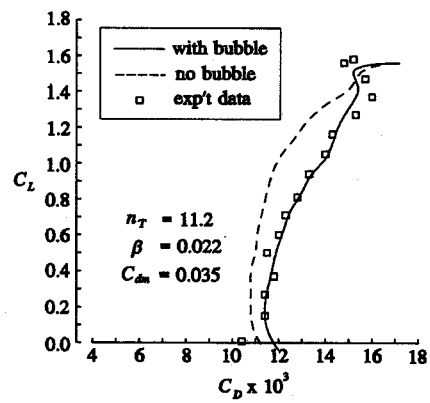

Fig. 6 FX 66-S-196 V1 airfoil at Re_c = 0.5 $\times$ 10^6.

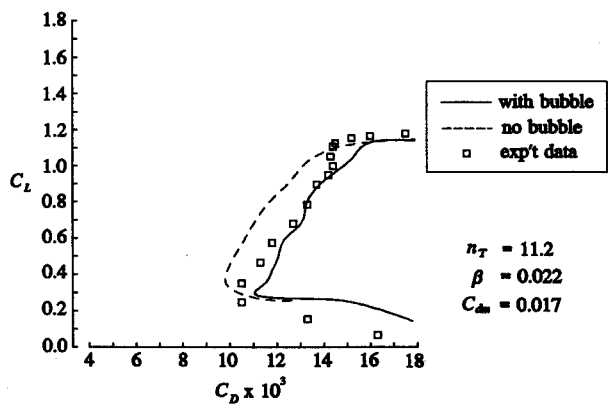

Fig. 7 Eppler 387 airfoil at Re_c = 0.2 $\times$ 10^6.

Table 1 Calculated Λ_R ranges for various airfoils with $\beta = 0.022$

Airfoil, $Re_c/10^6$	C_{dm}	Maximum Λ_R, @ l	Minimum Λ_R, @ l
Eppler 387[a] (0.2)	0.017	−0.0069 (0.18)	−0.0074 (0.34)
Eppler 387[a] (0.3)	0.025	−0.0071 (0.12)	−0.0076 (0.20)
FX 66-S-196 VI[b] (0.5)	0.035	−0.0075 (0.06)	−0.0090 (0.13)
FX 66-17A-175[c] (1.0)	0.055	−0.0081 (0.05)	−0.0088 (0.07)
FX 66-17A-175[c] (1.5)	0.075	−0.0081 (0.04)	−0.0086 (0.05)
Eppler 403[c] (1.0)	0.055	−0.0069 (0.05)	−0.0102[d] (0.12)
UAG 88-143/20[c] (0.69)	0.043	−0.0071 (0.07)	−0.0106[d] (0.15)
FX LV-152[c] (0.5)	0.035	−0.0071 (0.08)	−0.0089 (0.21)

[a]NASA Langley Low-Turbulence Pressure Tunnel, $n_T = 11.2$. [b]Low Speed Laboratory of the Delft University of Technology, $n_T = 11.2$. [c]Laminar Wind Tunnel at the University of Stuttgart, $n_T = 14$. [d]Out of suggested range ($-0.0060 > \Lambda_R > -0.0099$).

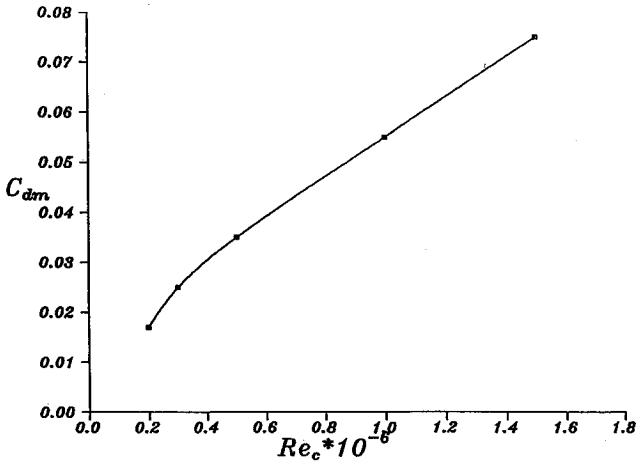

Fig. 8 Correlations between C_{dm} and Re_c.

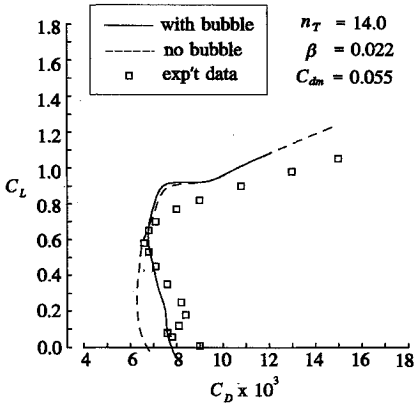

Fig. 9 Eppler 403 airfoil at $Re_c = 10^6$.

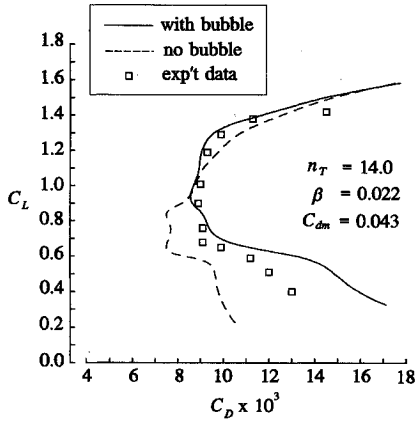

Fig. 10 UAG 88-143/20 airfoil at $Re_c = 0.69 \times 10^6$.

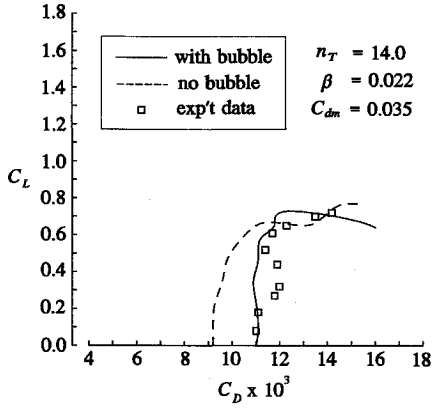

Fig. 11 FX LV 152 airfoil at $Re_c = 0.5 \times 10^6$.

After calibrating the bubble model with the above three sets of data, it is proposed that β has a universal value of 0.022 at all combinations of n_T and Re_c, whereas C_{dm} is dependent on Re_c only. As shown in Fig. 8, the correlations between C_{dm} and Re_c can be determined by fitting a cubic spline through the above findings.

The airfoils selected for verification include Eppler 403,[24] UAG 88-143/20,[25,26] and FX LV-152.[23] The bubbles on these three airfoils are dominant and should be able to illustrate the effectiveness of the current bubble model.

The Eppler 403 airfoil was tested at $Re_c = 10^6$ in Stuttgart LWT, so that n_T was chosen to be 14. As seen in Fig. 9, a major improvement in predicting the drag polar is obtained after the addition of the bubble model, although C_D is still underpredicted by about 0.0008 at $C_L = 0.2$. This underprediction is probably due to excessive bubble size (as long as 12% chord at $Re_c = 10^6$).

The UAG 88-143/20 airfoil might be the most challenging one of the selected three to simulate. To reduce drag, the airfoil was designed to have its pressure recovery at about 60% chord. Thus, the velocity gradient at separation is relatively high, resulting in a large separation bubble. Again, n_T was chosen as 14 because the airfoil was tested at Stuttgart LWT. It can be seen in Fig. 10 that the bubble model brings major improvement to the drag prediction at $Re_c = 0.69 \times 10^6$ when the bubble length can extend to about 10% chord.

The final airfoil to be verified against is FX LV-152, which is symmetric in shape. Figure 11 shows that dramatic improvement is obtained at $Re_c = 0.5 \times 10^6$ after the addition of the bubble model, although C_D is still underpredicted by 0.001 at $C_L = 0.35$. The calculation shows that at $C_L = 0.35$, the length on the upper surface bubble is 14% chord, while the bubble on lower surface has its length extended to 21% chord. It is likely that the underprediction of drag is due to the excessive bubble size on the lower surface.

As mentioned earlier, the theoretical value of Λ_R calculated from Eq. (12) can be used to check the validity of the bubble model. Table 1 shows the calculated Λ_R ranges for various airfoils with β set at 0.022. These data are gathered from

midchord bubbles only, but cover a wide range of bubble size and Re_c. Except for two cases in which the minimum Λ_R values are slightly out of range, all the other cases have Λ_R values well within the suggested range ($-0.0060 > \Lambda_R > -0.0099$) from Schmidt.[10] Therefore, 0.022 should be an appropriate value for β.

The calculation results suggest that the bubble model can indeed improve the drag prediction, especially when it is applied to the midchord bubble. Some improvements must be made on the calculation of l_1 before the bubble model can be applied to situations with Re_c less than 0.2×10^6.

Conclusions

A separation bubble model was developed and incorporated into an existing airfoil analysis program to improve its low Re_c prediction accuracy. Based on Horton's method, the model can be easily retrofitted to an existing boundary-layer code. Also, it requires minimal computation time, while producing results accurate for engineering purposes.

To improve the prediction accuracy, the original Horton's formulations were replaced with those which agree more closely with experimental observations on bubbles. Therefore, Van Ingen's and Schmidt's correlations were adopted for the calculation of the laminar region of the bubble, so that both the effect of freestream turbulence on transition and the substantial boundary-layer growth in the laminar region can be accounted for. The linear velocity distribution proposed by Horton was replaced by the concave velocity distribution resulting from Wortmann's optimum pressure recovery to produce a better simulation of the turbulent region of the bubble.

Besides functioning as a link between the laminar and turbulent boundary layers, the bubble model also acts as a bursting criterion. Testing with published data from various wind tunnels confirms that the bubble model can simulate midchord bubbles in the Re_c range between $0.2–1.5 \times 10^6$, with accuracy good enough for engineering purposes. Compared with other bubble models, the current one is probably the simplest available. This is because the calculation only involves parameters at three locations (separation, transition, and reattachment), thus avoiding the need of numerical integration between these points. Its simplicity even allows the current bubble model to be used in airfoil analysis on desktop computers.

Acknowledgment

This research was supported by the Natural Sciences and Engineering Research Council of Canada.

References

[1]Ward, J. W., "The Behaviour and Effects of Laminar Separation Bubbles on Aerofoils in Incompressible Flow," *Journal of the Royal Aeronautical Society*, Vol. 67, No. 636, 1963, pp. 783–790.

[2]Tani, I., "Low-Speed Flows Involving Bubble Separations," *Progress in Aeronautical Sciences*, Vol. 5, Pergamon Press, New York, 1964, pp. 70–103.

[3]Horstmann, K. H., Quast, A., and Boermans, L. M. M., "Pneumatic Turbulators—A Device for Drag Reduction at Reynolds Number Below 5×10^6," AGARD CP 365, May 1984, pp. 20-1–20-19.

[4]Marsden, D. J., "A High-Lift Wing Section for Light Aircraft," *Canadian Aeronautics and Space Journal*," Vol. 34, No. 1, 1988, pp. 55–61.

[5]Drela, M., "Low Reynolds-Number Airfoil Design for the M.I.T. Daedalus Prototype: A Case Study," *Journal of Aircraft*, Vol. 25, No. 8, 1988, pp. 724–732.

[6]Horton, H. P., "A Semi-Empirical Theory for the Growth and Bursting of Laminar Separation Bubbles," Aeronautical Research Council, Britain, Current Paper 1073, June 1967.

[7]Van Ingen, J. L., "Transition, Pressure Gradient, Suction, Separation and Stability Theory," AGARD CP 224, 1977, pp. 20-1–20-15.

[8]Van Ingen, J. L., and Boermans, L. M. M., "Aerodynamics at Low Reynolds Numbers: A Review of Theoretical and Experimental Research at Delft University of Technology," *Proceedings of the International Conference on Aerodynamics at Low Reynolds Numbers*, Vol. I, Royal Aeronautical Society, London, 1986, pp. 1.1–1.40.

[9]Gleyzes, C., Cousteix, J., and Bonnet, J. L., "A Calculation Method of Leading Edge Separation Bubbles," II Symposium on Numerical and Physical Aspects of Aerodynamics Flows, Long Beach, CA, Jan. 1983.

[10]Schmidt, G. S., and Mueller, T. J., "Analysis of Low Reynolds Number Separation Bubbles Using Semiempirical Methods," *AIAA Journal*, Vol. 27, No. 8, 1989, pp. 993–1001.

[11]Stratford, B. S., "The Prediction of Separation of the Turbulant Boundary Layer," *Journal of Fluid Mechanics*, Vol. 5, Jan. 1959, pp. 1–16.

[12]Stratford, B. S., "An Experimental Flow with Zero Skin Friction Throughout its Region of Pressure Rise," *Journal of Fluid Mechanics*, Vol. 5, Jan. 1959, pp. 17–35.

[13]Wortmann, F. X., "A Contribution to the Design of Laminar Profiles for Gliders and Helicopters," *Zeitschrift für Flugwissenshaften*, Vol. 3, No. 10, 1955, pp. 333–345; also in translation, Great Britain, Ministry of Aviation TIL/T.A903, 1960.

[14]Roberts, W. B., "Calculation of Laminar Separation Bubbles and Their Effect on Airfoil Performance," *AIAA Journal*, Vol. 18, No. 1, 1980, pp. 25–31.

[15]Drela, M., and Giles, M. B., "ISES: A Two-Dimensional Viscous Aerodynamic Design and Analysis Code," AIAA Paper 87-0424, 1987.

[16]Dini, P., "A Computationally Efficient Modelling of Laminar Separation Bubbles," Ph.D. Dissertation, Pennsylvania State Univ., University Park, PA, 1990.

[17]Kennedy, J. L., "The Design and Analysis of Airfoil Sections," Ph.D. Dissertation, University of Alberta, Edmonton, Alberta, Canada, April 1977.

[18]Eppler, R., "Practische Berechnung Laminarer und Turbulenter Absuage Grenzschichten," Ingenieur Archiv, Bd. 32, 1963, pp. 222–245.

[19]Lui, C. V., and Sandborn, V. A., "Evaluation of the Separation Properties of Laminar Boundary Layers," *Aeronautical Quarterly*, Vol. 19, Aug. 1968, pp. 235–242.

[20]Curle, N., and Skan, S. W., "Approximate Methods for Predicting Separation Properties of Laminar Boundary Layers," *Aeronautical Quarterly*, Vol. 8, 1957, pp. 257–268.

[21]Squire, H. B., and Young, A. D., "The Calculation of the Profile Drag of Aerofoils," Aeronautical Research Council R & M 1838, 1937.

[22]McGhee, R. J., Walker, B. S., and Millard, B. F., "Experimental Results for the Eppler 387 Airfoil at Low Reynolds Number in the Langley Low-Turbulence Pressure Tunnel," NASA TM 4062, 1988.

[23]Althaus, D., and Wortmann, F. X., *Stuggarter Profilkatalog I*, Univ. of Stuttgart, Stuttgart, Germany, 1972.

[24]Eppler, R., *Airfoil Design and Data*, Springer-Verlag, Berlin, 1990.

[25]Marsden, D. J., "Wind Tunnel Tests of an Ultralight Sailplane Wing Section," *Technical Soaring*, Vol. XIV, No. 1, 1990, pp. 7–12.

[26]Althaus, D., and Würz, W., "Wind Tunnel Tests of the UAG 88-143/20 Airfoil," Univ. of Stuttgart Internal Rept., Stuttgart, Germany, June 1991.